Biogeosciences Discuss., 9, 18865–18906, 2012
www.biogeosciences-discuss.net/9/18865/2012/
doi:10.5194/bgd-9-18865-2012

Biogeosciences Discussions

Si cycling in a forest biogeosystem – the importance of anthropogenic perturbation and induced transient state of biogenic Si pools

M. Sommer[1,2], H. Jochheim[3], A. Höhn[1], J. Breuer[4], Z. Zagorski[5], J. Busse[6], D. Barkusky[7], D. Puppe[1,8], M. Wanner[8], and D. Kaczorek[1,5]

[1]Leibniz-Centre for Agricultural Landscape Research, Institute of Soil Landscape Research, Eberswalder Str. 84, 15374 Müncheberg, Germany
[2]University of Potsdam, Institute of Earth and Environmental Sciences, Karl-Liebknecht-Str. 24–25, 14476 Potsdam, Germany
[3]Leibniz-Centre for Agricultural Landscape Research, Institute of Landscape System Analysis, Eberswalder Str. 84, 15374 Müncheberg, Germany
[4]Landwirtschaftliches Technologiezentrum Augustenberg (LTZ), Referat 12, Neßlerstr. 23–32, 76227 Karlsruhe, Germany
[5]Department of Soil Environment Sciences, Warsaw University of Life Science (SGGW), Nowoursynowska 159, 02-776 Warsaw, Poland
[6]Leibniz-Centre for Agricultural Landscape Research, Institute of Landscape Biogeochemistry, Eberswalder Str. 84, 15374 Müncheberg, Germany

[7]Leibniz-Centre for Agricultural Landscape Research, Research Station Müncheberg, Eberswalder Str. 84, 15374 Müncheberg, Germany
[8]Brandenburg University of Technology Cottbus, Chair General Ecology, 03013 Cottbus, Germany

Received: 30 September 2012 – Accepted: 19 November 2012
– Published: 19 December 2012

Correspondence to: M. Sommer (sommer@zalf.de) and H. Jochheim (hjochheim@zalf.de)

Published by Copernicus Publications on behalf of the European Geosciences Union.

BGD
9, 18865–18906, 2012

Abstract

The relevance of biological Si cycling for dissolved silica (DSi) export from terrestrial biogeosystems is still in debate. Even in systems showing a high content of weatherable minerals, like Cambisols on volcanic tuff, biogenic Si (BSi) might contribute > 50 % to total DSi (Gerard et al., 2008). However, the actual number of biogeosystem studies is rather limited for generalised conclusions. To cover one end of controlling factors on DSi – weatherable minerals content – we studied a forested site with absolute quartz dominance (> 95 %). Hence, we hypothesise minimal effects of chemical weathering of silicates on DSi. During a four year observation period (May 2007–April 2011) we quantified (i) internal and external Si fluxes of a temperate-humid biogeosystem (beech, 120 yr) by BIOME-BGC (vers. ZALF), (ii) related Si budgets, and, (iii) Si pools in soil and beech, chemically as well as by SEM-EDX. For the first time both compartments of biogenic Si in soils were analysed, i.e. phytogenic and zoogenic Si pool (testate amoebae). We quantified an average Si plant uptake of 35 kg Si ha^{-1} yr^{-1} – most of which is recycled to the soil by litterfall – and calculated an annual biosilicification from idiosomic testate amoebae of 17 kg Si ha^{-1}. High DSi concentrations (6 mg l^{-1}) and DSi exports (12 kg Si ha^{-1} yr^{-1}) could not be explained by chemical weathering of feldspars or quartz dissolution. Instead, dissolution of a relictic phytolith Si pool seems to be the main process for the DSi observed. We identified forest management, i.e. selective extraction of pine trees 20 yr ago followed by a disappearance of grasses, as the most probable control for the phenomena observed and hypothesised the biogeosystem to be in a transient state in terms of Si cycling.

1 Introduction

In recent years our understanding on Si in terrestrial biogeosystems has been improved substantially. Methodological progress for a quantification of Si pools in soils, plants and waters have been achieved by emerging Si isotopes techniques. Nowadays

BGD
9, 18865–18906, 2012

we are able to characterise isotopic signatures of different phases in soils in situ (Steinhoefel et al., 2011) and identify sources of soils' isotopic signature as well as biogenic (BSi) and dissolved Si (DSi) (Bern et al., 2010; Cornelis et al., 2010b; Engström et al., 2010; Opfergelt et al., 2010). Furthermore, our understanding of important fractionation processes in the soil-plant system has advanced (Ding et al., 2008; Delstanche et al., 2009). Chemical extraction procedures for Si pools in soils were developed and applied to different soils, mainly focusing on amorphous Si (ASi) (Saccone et al., 2007; Höhn et al., 2008; Guntzer et al., 2010; Cornelis et al., 2011a). Experimental setups for phytolith dissolution were established (Fraysse et al., 2009, 2010) and pedon scale modeling of the Si cycling has been improved (Gerard et al., 2008).

Research on steppe (Blecker et al., 2006; Borrelli et al., 2010) and savannah biogeosystems (Melzer et al., 2010, 2012; Alexandre et al., 2011) as well as wetlands (Struyf and Conley, 2009; Struyf et al., 2009) complements our understanding on the "plant factor", i.e. the importance of the biological Si cycling in terrestrial biogeosystems which had been studied in tropical and temperate climates so far (Sommer et al., 2006). The complex effects of perturbations, like deforestation (Conley et al., 2008), invading insects (Grady et al., 2007), or fire (Engle et al., 2008) on DSi exports from catchments challenges the steady state assumption implied in most studies on Si budgets.

Although a spatial hierarchy of driving factors for DSi exports is well known (Sommer et al., 2006; Cornelis et al., 2011b) the origin of DSi is still in debate. The major research questions in respect to Si cycling in terrestrial biogeosystems are: How large is the contribution of BSi pool to DSi compared to litho-/pedogenic sources? And: what are the main drivers of the relative importance of biogenic and mineral sources – climate, lithology, stage of soil development, soil pattern, land use? To answer these questions Cornelis et al. (2011b) developed a conceptual framework. They defined four different scenarios ("end members") based on climate (runoff, temperature), soil conditions (weatherable minerals) and Si recycling by vegetation. Each scenario should be reflected by characteristic DSi geochemical signatures (δ^{30}Si, Ge/Si) which can be used in tracing biogeochemical Si cycle of soil-plant systems. Generally these signatures

BGD
9, 18865–18906, 2012

have to be combined with Si flux analysis (incl. mass balances) and Si pool quantifications in order to understand the fate of Si in terrestrial biogeosystems. However, the number of studies in which Si fluxes in/from the soil-plant system are directly linked to a detailed analysis of Si pools is still limited (e.g. Alexandre et al., 1997; Lucas, 2003; Gerard et al., 2008). Furthermore, no study included zoogenic Si pool, although first results on testate amoebae dynamics already showed its relevance in terms of biosilicification (comparable to plants, Aoki et al., 2007).

Here we present results on Si cycling in a climate weathering-limited biogeosystem (in terminology of Cornelis et al., 2011b). We hypothesised that the effect of Si biocycling on DSi export must be most pronounced in cases of minimum intensity of chemical weathering. Therefore we selected a forested biogeosystem with quartz dominance in soils and parent material (> 95 %). Based on a system approach we quantified Si fluxes (internal, external) for a 4-yr period and interpreted DSi exports in terms of litho-/pedogenic and biogenic Si pools. For the first time the quantification of the biogenic Si pool comprises both, the phytogenic and zoogenic pool.

2 Materials and methods

2.1 Environmental setting

The study site "Beerenbusch" is located in Northern Brandenburg close to the village Rheinsberg (53.1° N, 13.0° E). It was established at a 0.5 ha fenced, almost flat area at 78 m a.s.l. The climate is characterised by mean annual air temperature of 8.7 °C and average precipitation of 600 mm yr^{-1}, according to long term measurements (1981–2010) of the meteorological station Neuglobsow/Menz of the German Weather Service (DWD) which is located at a distance of 6 km from the forest stand. The mean precipitation during the study period (May 2007–April 2011) was somewhat higher (689 mm).

The study site is located at a Weichselian outwash plain (sandur) of the Rheinsberg Basin in the foreland of Late Pleistocene terminal moraines ("Fürstenberger Staffel",

BGD
9, 18865–18906, 2012

Ginzel and Ertl, 2004). The soil is classified as *Brunic Arenosol (dystric)* according to WRB (2006) and *Lamellic Udipsamment* according to Soil Taxonomy (Soil Survey Staff, 1999). Humus enriched topsoils extend down to a depth of 35 cm. Bleached quartz grains indicate a slight podsolization for the first mineral horizon (AE). Brunification leads to a bright brownish colour in the subsoil (Bw horizons) down to a depth of 80 cm. Single thin clay lamellae in subsoil and parent material indicate clay translocation macroscopically (down to 120 cm).

The vegetation is characterised by a mature European beech (*Fagus sylvatica* L.) stand which was planted in 1888 under a pine forest (*Pinus sylvestris* L.). The upper pine layer of the mixed forest stand was cut step by step during the years 1985–88. In 2008 at the age of 120 yr the forest stand is characterised by a mean tree height of 27.6 m, a stem diameter at breast height of 36.8 cm, a ground base area of 26.6 $m^2\,ha^{-1}$, a tree number of 216 ha^{-1}, and a timber volume of 369 $m^3\,ha^{-1}$.

The recent plant community is classified as a *Majanthemo-Fagetum* with coverages of 85 % beech in the upperstorey, 5 % in the intermediate layer and 20 % in the understorey. The ground vegetation is dominated by herbs (1 % coverage), mosses (5 %), and lichens (< 1 %) (F. Becker, personal communication, 2004).

2.2 Sampling and analysis of soils, plants, phytoliths, and testate amoebae

A representative soil pit as well as a sediment core (5 m depth) had been analysed for basic textural and chemical properties prior to this study (Lachmann, 2002; Jochheim et al., 2007). The soil pit is located approx. 50 m apart from the location of the sediment core. Assuming a principally similar sediment layering we integrated results of both samplings into single depth functions (down to 2.8 m). For Si analysis a resampling from the original soil pit occurred end of September 2009.

Litter and soil material was taken by horizons down to a depth of 1.25 m and stored in plastic bags. Undisturbed soil cores (100 cm^3) were taken in the middle of soil horizons and dried at 105 °C for determination of bulk density (BD) (Lachmann, 2002). Bulk densities for sediments from core were estimated to be 1.7 $Mg\,m^{-3}$ (highest value

BGD
9, 18865–18906, 2012

of subsoil horizons) which probably represents the lower end of real values (= conservative estimate of true mass densities). Bulk soil samples were air dried, gently crushed and sieved at 2 mm to separate the fine earth fraction (< 2 mm) from gravel (> 2 mm). The particle size distribution of the fine earth was determined by a combined wet sieving (> 63 µm) and pipette (< 20 µm) method (DIN ISO 11277, 1998). Pretreatment for particle size analysis was done by wet oxidation of organic matter using H_2O_2 (10 Vol. %) at 80 °C and dispersion by shaking the sample end over end for 16 h with a 0.01 M $Na_4P_2O_7$-solution (Schlichting et al., 1995). Soil pH was measured using a glass electrode in 0.01 M $CaCl_2$ suspensions at a soil to solution ratio of 1 : 5 (w/v) (DIN ISO 10390, 1997) after a 60 min equilibration period. The total carbon content was determined by dry combustion using an elemental analyser (Vario EL, Elementar Analysensysteme, Hanau, Germany). $CaCO_3$ was determined conductometrically following Scheibler (Schlichting et al., 1995). Organic carbon (C_{org}) was calculated as the difference between total carbon and carbonate carbon. In soil horizons and sediments without carbonates total carbon equals soil organic carbon. Pedogenic oxides were characterised by dithionite-soluble (DCB) Fe (Fe_d) and dark acid-oxalate soluble Fe, Al, and Si (Al_o, Fe_o, Si_o) following the procedures of Mehra and Jackson (1960) and Schwertmann (1964), respectively (Schlichting et al., 1995). The element concentrations in solutions were determined by ICP-OES. All basic soil analyses were performed in two lab replicates.

2.2.1 Water extractable Si (Si_{H_2O})

The determination of water extractable Si based on the method described by Schachtschabel and Heinemann (1967). Ten grams of dry soil (< 2 mm) were weighted into 80 ml plastic centrifuge tubes and 50 ml distilled water added with three drops of a 0.1 % NaN_3-solution to prevent microbial activity. The total extraction time was seven days and the tubes were shaken by hand twice a day. The samples were not shaken mechanically to avoid abrasion of coarse mineral particles colliding during shaking (Mc Keague and Cline, 1963). Finally the extraction solution was centrifuged (4000 rpm,

BGD
9, 18865–18906, 2012

20 min), filtrated (0.45 µm polyamide membrane filters) and elements were measured by ICP-OES. Analyses were performed in three lab replicates.

2.2.2 Tiron extractable Si (Si_{Tiron})

The Tiron ($C_6H_4Na_2O_8S_2 \cdot H_2O$) extraction procedure was developed by Biermans and Baert (1977) and modified by Kodama and Ross (1991). It has been used to quantify "pedogenic silica" (Kendrick and Graham, 2004; Sauer et al., 2006). The extraction procedure is as follows: Dilution of 31.42 g Tiron (ACROS Organics, Geel, Belgium) with 800 ml of distilled water, followed by addition of 100 ml sodium carbonate-solution (5.3 g Na_2CO_3 in 100 ml distilled water) under constant stirring. After that the pH of the solution increases from 3.3 to 7.5. Finally the pH is brought to 10.5 by adding small volumes of a 4 M NaOH-solution. The Tiron-solution is transferred into a 1 l volumetric flask and has a final concentration of 0.1 M. For the extraction 30 mg of dry ground soil (< 0.180 mm) is weighted into 80 ml centrifuge tubes and a 30 ml aliquot of the Tiron-solution added. The tubes are then heated at 80 °C in a water bath for 1 h. After cooling adhering water on the surface of the tubes is removed, the tubes are weighted and water lost by evaporation is replaced. The extracted solutions were centrifuged at 4000 rpm for 30 min and filtered using 0.45 µm polyamide membrane filters (Whatman NL 17). Analyses were performed in three lab replicates.

2.2.3 Mineralogy, micromorphology and SEM-EDX analysis

Powder samples of each soil horizon (< 2 mm fraction) were analysed for basic mineral composition using a BRUCKER AXS D5000 Diffractometer (Cu-Kα radiation). The relative intensities of the diffraction maxima were used for a semiquantitative estimation of the concentration of mineral species present. The counts from the main reflection peak of all minerals were summed up and the relative proportion of each mineral was calculated as percent of the total. A subsample of < 2 mm fraction was placed on an Al-stub, fixed by adhesive tape, coated with minimal amount of gold-palladium and analysed

BGD
9, 18865–18906, 2012

on element composition by microprobe analysis (Hitachi S-2700 device, EDX-X-Flash-Detector with SAMX-Software at ZELMI, TU-Berlin).

Four undisturbed soil samples (Kubiena boxes of 8 cm height) were taken from 0–8 cm (AE, Ah), 10–18 cm (AB), 44–52 cm (Bw_1) and 104–112 cm (2Cwt). Air-dried samples were impregnated with Leguval resin under vacuum. After hardening 24 µm thick thin sections were prepared. The micromorphological features were described according to the concepts and terminology proposed by Stoops (2003). For thin section descriptions a SM-LUX-POL (Leitz) microscope with polarisation filter was used. After description thin sections were coated with carbon in a vacuum evaporator, and then examined with electron microprobe analyses (Cameca Camebax Microbeam, ZELMI at TU Berlin), using an accelerating potential of 20 kV. Element distribution maps (Si, Al, Fe, K, Mg, Ca, Na, Ti) were obtained with the same instrument. The identification of feldspar grains and cutans (Fig. 5) was done using microscopic examination of the four thin sections (between 10 and 20 replicates, depending on the number of feldspar grains in each thin section). To obtain information about the weathering state of potassium feldspars, strewn slides of soil material from three different depths (10–20, 40–60, and 100–130 cm) were prepared and analysed using SEM (Fig. 6). For identification of feldspars, samples were analysed with SEM-EDX and the potassium distribution in the slides was recorded. Each strewn slide was divided into four subsections and a minimum of ten replicates were analysed.

2.2.4 Phytolith separation from plants and soils, SEM-EDX analysis

Phytoliths were extracted from litterfall, the organic surface layer (L) as well as from the first three mineral horizons (AE, Ah, AB). Litterfall from one sampling date (May to August 2008) was separated into four groups: leaves, bud scale, cupules and wood from twigs and branches. The extraction procedure for litterfall was similar to soil horizons except steps 3 and 4 (see below). From each horizon 10 g of dry soil material (< 2 mm) were processed in four steps (adapted from lab manual of Anne Alexandre, CEREGE, Aix en Provence, France):

BGD
9, 18865–18906, 2012

1. Oxidation of organic matter using H_2O_2 (35 Vol. %), HNO_3 (65 Vol. %), $HClO_4$ (70 Vol. %) at 80 °C until reaction subsides,

2. Dissolution of carbonates and Fe oxides by boiling the sample in HCl (10 Vol. %) for 30 min,

3. Removal of the < 2 µm granulometric fraction: dispersion of remaining solid phase of step 2 with 2 Vol. % sodium hexametaphosphate solution (6–12 h), centrifugation at 1000 rpm for 2–3 min, and subsequent decantation,

4. Separation of the phytoliths: shaking of remaining solid phase of step 3 with 30 ml of sodium polytungstate $Na_6(H_2W_{12}O_{40})\cdot H_2O$ (density of 2.3 g cm^{-3}), centrifugation at 3000 rpm for 10 min, carefully pipetting the supernatant, and filtering by 5 µm teflon filter. This step was repeated three times. The filter residue was washed with water, bulked, dried at 105 °C, and weighted.

A subsample was placed on an Al-stub, fixed by adhesive tape, and coated with minimal amount of gold-palladium. 10 micrographs per stub were made using a JEOL JSM6060 LV SEM microscope (500× magnification). Phytoliths of each micrograph (coverage approx. 200 × 200 µm^2) were counted. The data base comprises a total number of 462 (L), 459 (AE), 422 (Ah), and 238 phytoliths (AB). They were described by size and shape (Madela et al., 2005) and assigned to vegetation (Golyeva, 2001) wherever applicable. Further, all counted phytoliths were assigned to one of three classes of phytolith dissolution: (i) plain phytoliths, (ii) phytoliths showing some surface etching, and, (iii) phytoliths with strong dissolution features. Phytoliths at stubs were analysed on element composition by microprobe analysis (Hitachi S-2700 device, EDX-X-Flash-Detector with SAMX-Software at ZELMI, TU Berlin).

2.2.5 Plant analysis

The collected plant litter (see 2.3) was oven-dried at 105 °C and milled in a planet type ball mill using milling vessels and balls made from ZrO_2. Sample aliquots of

BGD
9, 18865–18906, 2012

approximately 200 mg were digested under pressure in PFA digestion vessels using a mixture of 2.5 ml HNO_3 and 1 ml HF at 220 °C and approximately 100 bar (Ultra Clave II, MLS GmbH, Leutkirch, Germany). Silicon was measured by ICP-OES (Vista Pro, Varian Inc., Australia) using a HF-resistant sample introduction system, radial viewing of the plasma, and matrix matched external calibration.

2.2.6 Quantification of testate amoebae and related Si pool

For testate amoebae analysis 5 field replicates (20 cm × 20 cm) were placed randomly at Beerenbusch site avoiding stem near areas (April 2011). The litter layer (beech leaves) was removed and volumetric soil probing occurred in two segments, 0–2.5 cm and 2.5–5 cm (= sample volume of 1000 cm^3). Aliquots of 2 g were taken for amoebae analysis in the field and stored in 8 ml formalin (4 % aqueous formaldehyde solution). Total soil material of each depth increment and 20 cm × 20 cm area was oven-dried at 105 °C and weighted. Bulk densities were calculated by dividing total soil mass by sample volume (1000 cm^3). Testate amoebae were determined at species level and enumerated directly with an inverted microscope using stained (aniline blue) soil suspensions received from serial dilution (30–500 mg soil in 8 ml water per sample) as reported by Wanner (1999). Thereby we were able to distinguish between living individuals and empty tests. All species were assigned either to idiosomic or xenosomic amoebae taxa building up their tests from idiosomes (siliceous platelets synthesised by amoebae from H_4SiO_4 in soil solution) or xenosomes (extraneous materials such as mineral particles), respectively (e.g. Meisterfeld, 2002a,b). Idiosomic Si pools ($g\,m^{-2}$) of the upper 5 cm were calculated by (1) multiplying Si content of tests (Table 1 in Aoki et al., 2007) with counted individuals of each species, (2) multiplying these data with bulk densities and thickness (2.5 cm), and, (3) finally summing up both depth increments.

BGD
9, 18865–18906, 2012

2.3 Site instrumentation for flux determinations

The investigations of study site's water budgets started in May 2001. The instrumentation as well as results of the first 4 yr are described in Jochheim et al. (2007a). Precipitation was measured continuously at an open field located 500 m south of the study site using a heated rain gauge (F&C GmbH Gülzow). Gaps in the precipitation data were filled using open land precipitation data of the ICP Forests level II plot DE1202 and of the weather station in Neuglobsow/Menz of the German Weather Service (DWD) close to the study site. For silicon analysis (started in May 2007) precipitation water of two rain samplers (RS200, UMS GmbH, Munich; 314 cm^2 each) were collected weekly. Throughfall was measured continuously using a gutter of 0.8 m^2 area with a tipping bucket rain gauge. Additionally, weekly measurements were carried out using 15 rain samplers (see above). Stemflow was measured continuously at one stem with a tipping bucket rain gauge, and additional weekly on 4 stems by sampling the water in barrels. For silicon analysis the weekly samples of open land precipitation, throughfall, and stemflow were bulked to monthly samples. Si concentrations in all waters were determined by ICP-OES.

Litterfall was collected in 8 inverted pyramidal litter traps (0.25 m^2 each) bi-weekly during four years (May 2006–April 2010) and separated into leaves, flowers, bud scales, beechnuts, fruit capsules, and wood from twigs and branches. Each fraction was bulked into three periods per year (January–April, May–August, September–December). For silicon analysis see *Plant Analysis* in 2.2.

Soil solution was sampled using borosilicate suction probes (EcoTech Bonn GmbH) from 20, 70, and 250 cm soil depths (mean of 150 cm and 250 cm distance to stem, 4 replicates per depth and distance). The samples were collected by applying a suction of −30 kPa in 20 and 70 cm, and −35 kPa in 250 cm. Water was stored within the shafts of the suction probes and sampled bi-weekly. For silicon analysis the 4 field replicates per depth and distance were bulked. Si in soil water was measured by ICP-OES.

BGD
9, 18865–18906, 2012

Analysis of water content was conducted hourly at different distances to stem (50, 150, 250 cm) of one stem in soil depths 20, 70, and 250 using Theta-probes ML2 (Delta-T Devices Ltd Cambridge, UK). Additionally, close to two further trees using identical distances to stem soil moisture was measured bi-weekly using TDR-probes (FOM/m-TDR, EasyTest Lublin, Poland) at identical soil depths.

Xylem sap flux was measured continuously during the vegetation periods of 2002–2005 on ten selected trees in 1.3 m tree height using the method after Granier (1985) and calculated to representative stand canopy transpiration following Lüttschwager and Remus (2007).

Aboveground woody tree biomass and forest growth were calculated by measuring stem diameter at breast height and tree height of all 108 trees of the plot in spring of 2006, 2008, and 2010 using form factors derived from the beech yield table (Dittmar et al., 1986), wood density (Trendelenburg and Mayer-Wegelin, 1955), bark density (Dietz, 1975), and bark fractions (Altherr et al., 1974).

2.4 Calculation and modeling of Si fluxes

Deposition of Si was calculated from the open land precipitation. Si fluxes were calculated by multiplying water fluxes with Si concentrations. Stand precipitation equals the sum of Si fluxes in throughfall and stemflow, whereas leaching from canopy is the difference of Si fluxes in stand precipitation and open land precipitation. Silicon uptake equals the sum of Si fluxes in litter fall, leaching from canopy, and wood increment. Si export through harvest was calculated as a sum of current accumulation of Si in stem wood including bark.

The simulation of water budget was carried out with the dynamic model Biome-BGC (vers. ZALF; Jochheim et al., 2007b; Puhlmann and Jochheim, 2007) which is based on Biome-BGC (Thornton et al., 2002). The model runs in daily time steps. It was re-calibrated and validated on the basis of data from intensive forest monitoring sites (Jochheim et al., 2009) as well as on forest yield tables. For this application the model was calibrated based on the measurements of the stand started in 2001. Silicon fluxes

BGD
9, 18865–18906, 2012

through soil and with drainage water were calculated for four years (May 2007–April 2011) by multiplying the Si concentrations in soil water from suction probes with simulated soil water fluxes. Vertical distribution of passive Si uptake in soil was estimated from vertical distributed soil water uptake rates multiplied by Si concentrations in soil water. As the Si concentrations in soil water were analyzed in 3 soil depths only (20, 70, 250 cm), they were extrapolated to all other soil depths using the vertical distribution of water extractable Si.

3 Results

3.1 Basic soil properties and soil mineralogy

The studied soil is very sandy throughout showing a sand content > 85 % and a dominance of medium sand fraction (0.2–0.63 mm, Fig. 1). In the upper 50 cm a slight increase in silt can be observed. Clay content is always below 3 % with slightly higher values in the upper 1.5 m. The soil is decalcified down to a depth of 1.8 m (Fig. 1). Acidification leads to pH values between 4.3 and 4.5 in the upper 1.6 m. Below pH increase to > 7.0 due to carbonatic sediments (2–4 % $CaCO_3$). Quartz is the dominant mineral throughout the soil horizons and sediment layers (Table 1). Only minor additions of feldspars (orthoclase > plagioclase), pyroxene and calcite occured. Pedogenic oxides (Fe, Al) decreased from C-enriched surface horizons (upper 20 cm) to subsoil horizons as crystallinity of iron oxides increased ($Fe_o : Fe_d$ 0.6 → 0.2). The molar Si/Al ratios in oxalate-oxalic acid extracts ($Si_o : Al_o$) remained below 0.3 in all soil horizons rendering neoformation of short range order minerals, like allophane or imogolite ($Si/Al \approx 0.5$), hardly probable.

3.2 Si pools in soils

Water soluble Si shows (i) a maximum of 16 mg kg^{-1} in the upper 2 cm, (ii) a decrease to 4 mg kg^{-1} in subsoil horizons, and, (iii) a recurring increase in sediments containing

BGD
9, 18865–18906, 2012

carbonates (Fig. 1). These findings can be explained by a combined effect of pH (lowest quartz solubility at pH 4–5) and the size of biogenic Si pool in different horizons. The water-soluble Si pool down to 2.8 m equals 21 g Si m^{-2} (= 210 kg Si ha^{-1}). The uppermost meter contains 6 g Si m^{-2} (= 60 kg Si ha^{-1}).

Tiron extractions lead to Si contents three orders of magnitude higher compared to water soluble Si. The depth function of Tiron-soluble Si shows a continuous decrease from 3 g kg^{-1} in topsoil horizons to < 2 g kg^{-1} in deepest sediments. The highest content can be observed in the uppermost horizon (AE) which is most probably a result of dissolution of biogenic Si (Guntzer et al., 2010). The Tiron extractable Si pool down to 2.8 m equals 10 kg Si m^{-2} (= 100 Mg Si ha^{-1}). The uppermost meter contains 4 kg Si m^{-2} (= 40 Mg Si ha^{-1}).

3.2.1 Phytogenic Si pool in soil

Phytolith contents decrease from litter to mineral soil horizons by one order of magnitude (Table 2). The upper 20 cm of the soil contain 140 g phytoliths m^{-2} (= 1400 kg ha^{-1}). Assuming all phytoliths to consist of pure SiO_2 we calculated 66 g Si m^{-2} for the phytolith Si pool in the upper 20 cm (= 660 kg Si ha^{-1}). The total phytogenic Si pool in soils will be even higher, because only the > 5 µm fractions of soil horizons are quantified by the phytolith separation procedure (see 2.2). Consequently, Si pool calculations from "traditional" phytolith separation systematically underestimate total phytogenic Si pool. A comparison between the Si content in phytoliths and measured Si content of leaves supports this consideration: the calculated Si content of phytoliths (2.4 g kg^{-1}, Table 2) only comprises 55 % of the measured Si content in beech leaves (4.4 g kg^{-1}, May–August 2008). BSi in the < 2 µm fraction probably explains this difference, because this fraction is lost during extraction by dissolution. In their early work Wilding and Drees (1971) already quantified 50 % of total leaf opal (*Fagus grandifolia*) in the < 2 µm fraction (another 22 % in 2–5 µm). Further, Watteau and Villemin (2001) provided evidence for nm-size phytogenic Si granules in leaves and soils.

BGD
9, 18865–18906, 2012

The phytolith assemblage of soil horizons – as detectable by size and shape – shows a dominance of grass phytoliths in mineral soil horizons below 2 cm (Table 2). Pine and moss phytoliths (rounded particles, Al-rich) can be identified as well (Table 2, Fig. 2b). As there are no more pine and grasses growing at the study since approx. 20 yr these phytoliths comprise a relictic biogenic Si pool. Surprisingly, clearly identifiable beech phytoliths only account for a minor portion in the upper centimeters. Further, those forms isolated from litterfall (Fig. 2a) are hardly detectable in their orginal shape in the soil, even not in the upper 2 cm (Fig. 2b). From these findings a rapid fractional dissolution of recent beech phytoliths might be concluded. Nevertheless, one has to recognize that 50–75 % of all phytoliths counted cannot be assigned to any vegetation throughout the uppermost 20 cm of the soil (Table 2).

3.2.2 Zoogenic Si pool in soil

A total number of $6.1 \times 10^8\,m^{-2}$ testate amoebae (60 % living individuals) was determined in the upper 5 cm of the soil. This number lies in the range of published data (e.g. Aoki et al., 2007; Ehrmann et al., 2012; Wanner and Dunger, 2001). Approximately 50 % of all individuals (living and empty tests) belong to either idiosomic or xenosomic taxa of testate amoebae. Xenosomic taxa build up their tests from extraneous materials such as mineral soil particles. Dominant xenosomic taxa at our site are *Phryganella acropodia*, *Plagiopyxis declivis*, and *Centropyxis sphagnicola* (Fig. 3d). Dominant idiosomic taxa embrace *Trinema complanatum*, *Euglypha rotunda*, and *Trinema lineare* (Fig. 3a–c). Only idiosomic taxa can be regarded as a biogenic Si pool influencing dissolved Si (DSi), because they synthesise siliceous platelets for their tests from silica of the soil solution. Therefore we calculated the zoogenic Si pool only on basis of idiosome-producing amoebae and came up with $0.19\,g\,Si\,m^{-2}$ in the upper 5 cm of the soil (= $1.9\,kg\,Si\,ha^{-1}$, Table 3). Compared to soil's phytolith Si pool these numbers are two orders of magnitude lower.

BGD
9, 18865–18906, 2012

3.3 Si in aboveground plant biomass

Beech leaves showed highest Si concentrations followed by bark of branch and stem wood, bud scales, and fruit capsules (Table 4). Beechnuts and woody biomass without bark contain the lowest Si concentrations. Interannual variations in Si concentrations are largest in leaves, bud scales, and fruit capsules. In 2006 lowest Si concentrations in leaves were measured (7 g kg^{-1}), in litterfall of 2007 Si concentrations nearly doubled (13.6 g kg^{-1}) which might be an effect of the length of growing period (dry summer in 2006). In terms of intraannual variations a seasonal trend of Si concentrations can be observed in leaves: Si concentrations in early stages of vegetation development (May–August) were lowest (4.4–6.8 g kg^{-1}), whereas during autumn/winter (September–December) or winter/spring (January–April) Si concentrations range from 6 to 14 g kg^{-1} (depending on single year). Taking into account the biomass of each plant compartment the total Si pool in aboveground biomass summarises to 83 kg Si ha^{-1} (Table 4). The stem bark makes up the largest fraction (50 %) followed by leaves (36 %), branch bark (6 %), and stem wood (3 %).

3.4 Internal and external Si fluxes

Si uptake by plants contributes the largest internal Si flux in the biogeosystem (35 kg Si ha^{-1} yr^{-1}, Fig. 4). The major part is transported into the leaves (30 kg Si ha^{-1} yr^{-1}) rendering autumn litter fall the most important annual flux component to the soil. Minor fluxes are related to annual litterfall of twigs, bud scales, fruits, and flowers (4 kg Si ha^{-1} yr^{-1}) or dendromass increments (0.7 kg Si ha^{-1} yr^{-1}). Although the Si pool size of testate amoebae is very small their relevance for internal Si cycling cannot be neglected. Due to relatively short generation times of idiosome-producing amoebae, e.g. Euglyphida (2–16 days with about 12–130 generations yr^{-1}, Schönborn, 1975, 1982; Lousier, 1984; Aoki et al., 2007) the annual biosilicification by idiosomes might be in the order of the cumulative annual Si uptake by plants. Using a conservative estimate of 15 generations per year we calculated an annual biosilicification of

BGD
9, 18865–18906, 2012

17 kg Si ha^{-1} yr^{-1} (Si pool of living idiosomic taxa). The turnover rates of idiosomic Si pool must be much higher compared to phytolithic Si pool as can be deduced from (only) 47 % empty tests of total idiosomic Si pool. Consequently, testate amoebae can be regarded as a temporal Si pool on a very short time scale.

The total Si input with open land precipitation is rather low (< 1 kg Si ha^{-1} yr^{-1}) which fits to the data from literature (Sommer et al., 2006; Cornelis et al., 2011b). The Si export by seepage equals 12 kg Si ha^{-1} yr^{-1} showing average silica concentrations of approx. 6 mg Si l^{-1} (Table 5). The high temporal variability between years (CV = 50 – 64 %) are mainly the result of varying drainage (Table 5), while temporal variations in silica concentrations were rather small (CV increase with depth: 4 → 11 %). During the observation period no seasonal trend in silica concentrations could be found, like a temperature dependency reported by Gerard et al. (2002). Mean silica concentration increases only slightly from acid soil horizons (0.2 m, 0.7 m) to the calcareous parent material in 2.5 m (4.9 → 5.7 mg Si l^{-1}, Table 5). This increase goes along with an increase in the water-soluble Si fraction (Fig. 1). One might conclude the dramatic change in physico-chemical soil properties, e.g. pH (Fig. 1), to be of minor importance for silica concentrations.

We set the annual accumulation rate of Si in stem wood and bark (0.6 kg Si ha^{-1} yr^{-1}) as the (annual) harvest export. Although not realised yet, at the end of a rotation period stem harvest leads to a complete Si export of this compartment. By adding this Si export to seepage losses we come up with a gross Si loss of 13 kg Si ha^{-1} yr^{-1}. Taking into account the inputs by deposition our biogeosystem reveals a net loss of 12 kg Si ha^{-1} yr^{-1}.

4 Discussion

The low atmospheric Si input is in accordance with reported values from other forested biogeosystems (< 2 kg ha^{-1} yr^{-1}, Sommer et al., 2006; Cornelis et al., 2011b). Throughfall and stemflow can also be neglected in terms of Si fluxes. The small annual

BGD
9, 18865–18906, 2012

increase in Si stored in the vegetation (biomass increment = 0.7 kg Si ha^{-1} yr^{-1}) is lower compared to reported data (European beech = 3.5 kg Si ha^{-1} yr^{-1}, Cornelis et al., 2010a) which might be explained by the lower forest growth of our mature beech stand (120 yr). The Si uptake by beech (35 kg Si ha^{-1} yr^{-1}) and return flux by litterfall (34 kg Si ha^{-1} yr^{-1}) lies in the range of other European beech stands in temperate climates (19–47 kg Si ha^{-1} yr^{-1}: Pavlov, 1972; Bartoli and Souchier, 1978; Ellenberg et al., 1986; Cornelis et al., 2010a). We calculated an averaged passive Si-uptake of 17 kg Si ha^{-1} yr^{-1} as the product of vertically distributed mean Si concentrations and modeled transpiration flux (239 mm yr^{-1}). When compared to the measured Si-uptake of 34 kg Si ha^{-1} yr^{-1} an active uptake of 50 % of total uptake can be concluded.

Generally, the magnitude of Si uptake at Beerenbusch surprises, when considering the very low content of weatherable minerals in the rooting zone (soils, sediments). It corresponds to a high Si supply as reflected by silica concentrations of seepage waters (6 mg Si l^{-1}). In principal three Si release processes might cause the silica concentrations observed: (i) quartz dissolution, (ii) intense weathering of silicates, and, (iii) dissolution of the biogenic Si pool (non-steady state).

4.1 Quartz dissolution and silicate weathering

Quartz has a water solubility of 1–7 mg l^{-1} (36–250 µmol l^{-1}) depending on particle size and temperature (Iler, 1979; Bartoli and Wilding, 1980; Dove, 1995). The lower value is more realistic for soils. This is supported by soil water data from quartz-rich, non-redoximorphic soils developed on quarzitic or granitic lithologies in the Black Forest (Podzols, Cambisols) showing silica concentrations always < 2.5 mg l^{-1} (Sommer et al., 2006). Studies from tropical soils with absolute quartz dominance also confirm low silica concentrations in soil waters (< 1.2 mg Si l^{-1}: Cornu et al., 1998; Lucas, 2001; Patel-Sorentino et al., 2007; do Nasciemento et al., 2008). There are two reasons for observed lower in situ silica concentrations compared to lab experiments on pure phases: (i) lab studies on quartz dissolution kinetics mostly use probes ground to silt

BGD
9, 18865–18906, 2012

size with fresh surfaces and high surface : volume ratios compared to our site with sand as the dominating particle size class. (ii) Surface coatings (Fe oxides, organic matter) protect quartz grains from intense dissolution. Coatings occur at all depths in our soil as depicted in soil thin sections (Fig. 5, upper). They show dark to light brown colors and an average thickness of 10–20 µm. From EDX analysis of several coatings (Fig. 5 lower) two different mineral phases can be identified – an iron bearing oxyhydroxide, most probably goethite, and kaolinite. Subsoil horizons show a higher percentage of Fe in the coatings ("ferri-argillans", compare Chartres, 1987; Stoops, 2003; Li et al., 2008). Because plagioclase and quartz coatings showed a similar chemical composition they cannot be interpreted as weathering rinds. Instead, a vertical redistribution of fine material, i.e. clay translocation (see macroscopic lamellae in 2Cwt), combined with a µm-scale horizontal redistribution of fines during desiccation of water films around grains are the most probable explanations. From these findings we conclude that quartz dissolution will contribute only a minor fraction to the (high) silica concentrations observed.

Weatherable minerals (mainly K-feldspars) contribute only 3 % (average) to the mineral assemblage of our soil and sediments. Therefore the influence of feldspar weathering on silica concentrations in water is minimal in principal. Nevertheless, we checked feldspar weathering intensity by thin sections and SEM. In thin sections some feldspars have been found as part of compact multimineral sand grains, probably derived from glacier grinding of granites and subsequent glaciofluvial sorting processes. Here the accessible surface area for chemical weathering is limited. Further, single feldspar grains appear only slightly weathered in SEM micrographs and do not show any trend with depth (Fig. 6). Because the pedochemical environment should enhance acid hydrolysis, our results are surprising. Coatings on feldspar grains (Fig. 5) might explain in part this apparent contradiction. In summary, we exclude feldspar weathering as an explanatory process for the silica concentrations observed.

BGD
9, 18865–18906, 2012

4.2 Dissolution of biogenic Si pool

The biogenic Si pool contains the phytogenic and the zoogenic Si pool, both of which differ remarkably in dynamics and turnover rates. The annual biosilicification of idiosomic amoebae by binary fission adds up to 17 kg Si ha^{-1} which is in the order of magnitude of the Si flux by litterfall, hence phytogenic silicification. On the other hand the idiosomic Si pool of 2 kg Si ha^{-1} is comparatively small. Empty tests comprise only 40 % (0.8 kg Si ha^{-1}) of total idiosomic Si pool, while living amoebae make up 60 % (1.2 kg Si ha^{-1}). Together with a flux/pool ratio of 8 these findings lead to our conclusion of a very high solubility of the idiosomic Si pool. Therefore, turnover rates are too high for interannual pool changes to become relevant for DSi exports.

Annual biosilicification by plants sums up to 35 kg Si ha^{-1}, most of which is returned to the soil by litterfall. Compared to the phytolith Si pool of 660 kg Si ha^{-1} – which comprises only part of the total phytogenic Si pool – this flux is relatively small (flux/pool ratio = 0.05). Therefore decadal changes of phytogenic Si pools are relevant for DSi exports in principal. Early experiments on phytolith dissolution in distilled water showed silicic acid equilibrium concentrations of 2–10 mg Si l^{-1} (Bartoli and Wilding, 1980) depending on plant species as well as surface area. These concentrations were higher than those determined for quartz (1 mg Si l^{-1}), but lower than synthesised pure silica gels (56 mg Si l^{-1}). The latter might be closer to solubilities of nm-sized phytogenic Si. Recent experiments on the reactivity of plant phytoliths in soil solutions have shown the solubility product to be close to that of amorphous silica and up to one order of magnitude higher than those of clay minerals (Fraysse et al., 2009, 2010). Half-life times of the studied phytoliths range from 10–12 yr (pH < 3) to < 1 yr (pH > 6). From these studies it is concluded that phytoliths represent a very reactive Si pool in soil solutions which contributes substantially to DSi.

To check status of phytolith dissolution in our soil we defined three classes of increasing dissolution and counted assigned phytoliths in SEM micrographs (Fig. 7). The percentage of plain phytoliths which show no signs of dissolution or surface etching

BGD
9, 18865–18906, 2012

decreases significantly from 69 % at soil surface down to 31 % in AB horizon (10–20 cm). Simultaneously phytoliths showing slight surface etching increased to 54 % while strongly dissoluted phytoliths had a maximum of 19 % in Ah (2–10 cm), but no clear depth trend. Combining these findings with (i) the observation of missing fresh beech phytoliths in soil horizons (see 3.2), and, (ii) the parallel increase of water-soluble Si with phytolith Si pool we regard dissolution of phytogenic Si as the most important driver of (high) DSi observed. This conclusion is indirectly supported by process-based modeling of the Si cycle in a forest biogeosystem (Gerard et al., 2008). In a Cambisol from volcanic tuff – containing much lower quartz (30 %) and higher percentages of clays and weatherable minerals (K-feldspars) compared to our site – the BSi account for 60 % of DSi after all.

Finally, as grasses – which are absent at recent beech stand – contribute a major part to recent phytolith pool we hypothesise the phytogenic Si pool of our soil not to be in steady state, but transient state: the continuous decomposition of the relictic phytogenic Si pool is actually not compensated by an equivalent upbuilding.

5 Conclusions

Our studied forest biogeosystem exhibits surprisingly high DSi concentrations and exports in relation to the very low content of weatherable minerals in soil and sediments. From our findings we excluded geochemical weathering processes as a major control on DSi, but concluded a strong biotic footprint on DSi. This has to be confirmed by Si isotope analysis of different phases, determination of Ge/Si ratios, and phytolith dissolution experiments in future research. Changes in forest management, i.e. the selective removal of pine trees 20 yr ago and concomitant disappearance of grasses in the understorey, seem to be the ultimate reason for the phenomena observed: the related phytogenic Si pool is in disequilibrium with recent vegetation and dissolving successively. We regard our study as another example highlighting the importance of perturbations in Si cycling (Ittekot et al., 2006; Laruelle et al., 2009; Struyf et al., 2009;

BGD
9, 18865–18906, 2012

Clymans et al., 2011; Struyf and Conley, 2012). Future research on Si cycling should consider decadal transient states more than to date.

Acknowledgements. The authors would like to thank Angela Müsebeck, Matthias Lemme, Regina Richter, Jürgen Beutler, and Michael Bähr for technical assistance and collecting samples at Beerenbusch, Dagmar Schulz for chemical analysis of samples, Dietmar Lüttschwager for providing data on sap flow analyses. Martin Kaupenjohann (TU Berlin), Francois Galbert and Jörg Nissen supported and performed EDX analysis at ZELMI (TU Berlin). Alexandra Golyeva and Chad Yost from the *Phy-Talk* forum provided help in identifying vegetation from phytoliths. This study was funded by the German Research Foundation (DFG) – PAK 179 "Multiscale analysis of Si cycling in terrestrial biogeosystems".

References

Alexandre, A., Meunier, J. D., Colin, F., and Koud, J. M.: Plant impact on the biogeochemical cycle of silicon and related weathering processes, Geochim. Cosmochim. Ac., 61, 677–682, 1997.

Alexandre, A., Bouvet, M., and Abbadie, L.: The role of savannas in the terrestrial Si cycle: A case study from Lamto, Ivory Coast, Global Planet. Change, 78, 162–169, 2011.

Altherr, E., Unfried, P., Hradetzky, J., and Hradetzky, V.: Statistische Rindenbeziehungen als Hilfsmittel zur Ausformung und Aufmessung unentrindeten Stammholzes, Mitteilungen der Forstlichen Versuch- und Forschungsanstalt Baden-Württemberg, 61, 1–137, 1974.

Aoki, Y., Hoshino, M., and Matsubara, T.: Silica and *testate amoebae* in a soil under pine-oak forest, Geoderma, 141, 29–35, 2007.

Bartoli, F. and Souchier, B.: Cycle et role du silicium d'origine végétale dans les écosystemes forestiers tempéres, Ann. Sci. Forest., 35, 187–202, 1978.

Bartoli, F. and Wilding, L. P.: Dissolution of biogenic opal as a function of its physical and chemical properties, Soil Sci. Soc. Am. J., 44, 873–878, 1980.

Bern, C. R., Brzezinski, M. A., Beucher, C., Ziegler, K., and Chadwick, O. A.: Weathering, dust, and biocycling effects on soil silicon isotope ratios, Geochim. Cosmochim. Ac., 74, 876–889, 2010.

Biermans, V. and Baert, L.: Selective extraction of the amorphous Al, Fe and Si oxides using an alkaline Tiron solution, Clay Miner., 12, 127–135, 1977.

BGD

9, 18865–18906, 2012

Blecker, S. W., McCulley, R. L., Chadwick, O. A., and Kelly, E. F.: Biologic cycling of silica across a grassland bioclimosequence, Global Biogeochem. Cy., 20, GB3023, doi:10.1029/2006GB002690, 2006.

Borrelli, N., Alvarez, M. F., Osterrieth, M. L., and Marcovecchio, J. E.: Silica content in soil solution and its relation with phytolith weathering and silica biogeochemical cycle in Typical Argiudolls of the Pampean Plain, Argentina – a preliminary study, J. Soils Sediments, 10, 983–994, 2010.

Chartres, C. J.: The composition and formation of grainy void cutans in some soils with textural contrast in Southeastern Australia, Geoderma, 39, 209–233, 1987.

Clymans, W., Struyf, E., Govers, G., Vandevenne, F., and Conley, D. J.: Anthropogenic impact on amorphous silica pools in temperate soils, Biogeosciences, 8, 2281–2293, doi:10.5194/bg-8-2281-2011, 2011.

Conley, D. J., Likens, G. E., Buso, D. C., Saccone, L., Bailey, S. W., and Johnson, C. E.: Deforestation causes increased dissolved silicate losses in the Hubbard Brook Experimental Forest, Global Change Biol., 14, 2548–2554, 2008.

Cornelis, J. T., Ranger, J., Iserentant, A., and Delvaux, B.: Tree species impact the terrestrial cycle of silicon through various uptakes, Biogeochemistry, 97, 231–245, 2010a.

Cornelis, J. T., Delvaux, B., Cardinal, D., Andre, L., Ranger, J., and Opfergelt, S.: Tracing mechanisms controlling the release of dissolved silicon in forest soil solutions using Si isotopes and Ge/Si ratios, Geochim. Cosmochim. Ac., 74, 3913–3924, 2010b.

Cornelis, J. T., Titeux, H., Ranger, J., and Delvaux, B.: Identification and distribution of the readily soluble silicon pool in a temperate forest below three distinct tree species, Plant Soil, 342, 369–378, 2011a.

Cornelis, J.-T., Delvaux, B., Georg, R. B., Lucas, Y., Ranger, J., and Opfergelt, S.: Tracing the origin of dissolved silicon transferred from various soil-plant systems towards rivers: a review, Biogeosciences, 8, 89–112, doi:10.5194/bg-8-89-2011, 2011b.

Cornu, S., Lucas, Y., Ambrosi, J. P., and Desjardins, T.: Transfer of dissolved Al, Fe and Si in two Amazonian forest environments in Brazil, Eur. J. Soil Sci., 49, 377–384, 1998.

Delstanche, S., Opfergelt, S., Cardinal, D., Elsass, F., Andre, L., and Delvaux, B.: Silicon isotopic fractionation during adsorption of aqueous monosilicic acid onto iron oxide, Geochim. Cosmochim. Ac., 73, 923–934, 2009.

Dietz, P.: Dichte und Rindengehalt von Industrieholz, Holz als Roh-und Werkstoff, 33, 135–141, 1975.

BGD
9, 18865–18906, 2012

DIN ISO 1039: Bodenbeschaffenheit: Bestimmung des pH-Wertes, Deutsches Institut für Normung, Beuth, Berlin, 1997.
DIN ISO 11277: Bodenbeschaffenheit: Bestimmung der Partikelgrößenverteilung in Mineralböden – Verfahren mittels Siebung und Sedimentation, Deutsches Institut für Normung, Beuth, Berlin, 1998.
Ding, T. P., Zhou, J. X., Wan, D. F., Chen, Z. Y., Wang, C. Y., and Zhang, F.: Silicon isotope fractionation in bamboo and its significance to the biogeochemical cycle of silicon, Geochim. Cosmochim. Ac., 72, 1381–1395, 2009.
Dittmar, O., Knapp, E., and Lembcke, G.: DDR-Buchenertragstafel 1983, Institut für Forstwissenschaften Eberswalde, Eberswalde, 1986.
Do Nascimento, N. R., Fritsch, E., Bueno, G. T., Bardy, M., Grimaldi, C., and Melfi, A. J.: Podzolization as a deferralitization process: dynamics and chemistry of ground and surface waters in an Acrisol – Podzol sequence of the upper Amazon Basin, Eur. J. Soil Sci., 59, 911–924, 2008.
Dove, P. M.: Kinetic and thermodynamic controls on silica reactivity in weathering environments, in: Chemical weathering rates of silicate minerals, Mineralogical Society of America and the Geochemical Society, Rev. Mineral. Geochem., 31, 235–290, 1995.
Ehrmann, O., Puppe, D., Wanner, M., Kaczorek, D., and Sommer, M.: *Testate amoebae* in 31 mature forest ecosystems – densities and micro-distribution in soils, Eur. J. Protistol., 48, 161–168, doi:10.1016/j.ejop.2012.01.003, 2012.
Ellenberg, H., Mayer, R., and Schauermann, J.: Ökosystemforschung – Ergebnisse des Sollingprojekts 1966–1986, Verlag Eugen Ulmer, Stuttgart, 1986.
Engle, D. L., Sickman, J. O., Moore, C. M., Esperanza, A. M., Melack, J. M., and Keeley, J. E.: Biogeochemical legacy of prescribed fire in a giant sequoia-mixed conifer forest: A 16-year record of watershed balances, J. Geophys. Res., 113, G01014, doi:10.1029/2006JG000391, 2008.
Engström, E., Rodushkin, I., Ingri, J., Baxter, D. C., Ecke, F., Österlund, H., and Öhlander, B.: Temporal isotopic variations of dissolved silicon in a pristine boreal river, Chem. Geol., 271, 142–152, 2010.
Fraysse, F., Pokrovsky, O. S., Schott, J., and Meunier, J.-D.: Surface chemistry and reactivity of plant phytoliths in aqueous solutions, Chem. Geol., 258, 197–206, 2009.
Fraysse, F., Pokrovsky, O. S., and Meunier, J.-D.: Experimental study of terrestrial plant litter interaction with aqueous solutions, Geochim. Cosmochim. Ac., 74, 70–84, 2010.

BGD
9, 18865–18906, 2012

Gerard, F., Francois, M., and Ranger, J.: Processes controlling silica concentration in leaching and capillary soil solutions of an acidic brown forest soil (Rhone, France), Geoderma, 107, 197–226, 2002.
Gerard, F., Mayer, K. U., Hodson, M. J., and Ranger, J.: Modelling the biogeochemical cycle of silicon in soils: application to a temperate forest ecosystem, Geochim. Cosmochim. Ac., 72, 741–758, 2008.
Ginzel, G. and Ertl, C.: Geologie, Hydrologie und Klima, in: Das Naturschutzgebiet Stechlin, edited by: Lütkepohl, M. and Flade, M., Natur & Text in Brandenburg, Rangsdorf, 15–23, 2004.
Golyeva, A.: Phytoliths and their information role in natural and archaeological objects, Syktyvkar Elista, Moscow, 2001.
Grady, A. E., Scanlon, T. M., and Galloway, J. N.: Declines in dissolved silica concentrations in western Virginia streams (1988–2003): Gypsy moth defoliation stimulates diatoms? J. Geophys. Res., 112, G01009, doi:10.1029/2006JG000251, 2007.
Granier, A.: Une novelle methode pour la mesure du flux de serve brute dans le tronc des arbres, Ann. Sci. Forest., 42, 193–200, 1985.
Guntzer, F., Keller, C., and Meunier, J.-D.: Determination of the silicon concentration in plant material using Tiron extraction, New Phytol., 188, 902–906, 2010.
Höhn, A., Sommer, M., Kaczorek, D., Schalitz, G., and Breuer, J.: Silicon fractions in Histosols and Gleysols of a temperate grassland site, J. Plant Nutr. Soil Sci., 171, 409–418, 2008.
Iler, R. K.: The chemistry of silica, Wiley-Interscience, New York, 1979.
Ittekot, V., Unger, D., Humborg, C., and Tac An, N. (Eds.): The silicon cycle – Human perturbations and impacts on aquatic systems, SCOPE 66, Island Press, Washington, 2006.
Jochheim, H., Einert, P., Ende, H.-P., Kallweit, R., Lüttschwager, D., and Schindler, U.: Wasser- und Stoffhaushalt eines Buchen-Altbestandes im Nordostdeutschen Tiefland – Ergebnisse einer 4jährigen Messperiode, Archiv für Forstwesen und Landschaftsökologie, 41, 1–14, 2007a.
Jochheim, H., Puhlmann, M., and Pohle, D.: Implementation of a forest management module into BIOME-BGC and its application, EOS Transactions Supplement, 88, B24A-04, 2007b.
Jochheim, H., Puhlmann, M., Beese, F., Berthold, D., Einert, P., Kallweit, R., Konopatzky, A., Meesenburg, H., Meiwes, K. J., Raspe, S., Schulte-Bisping, H., and Schulz, C.: Modelling the carbon budget of intensive forest monitoring sites in Germany using the simulation model BIOME-BGC, iForest, Biogeosci. For., 2, 7–10, 2009.

BGD
9, 18865–18906, 2012

Kendrick, K. J. and Graham, R. C.: Pedogenic silica accumulation in chronosequence soils, Southern California, Soil Sci. Soc. Am. J., 68, 1295–1303, 2004.
Kodama, H. and Ross, G. J.: Tiron dissolution method used to remove and characterize inorganic components in soils, Soil Sci. Soc. Am. J., 55, 1180–1187, 1991.
Lachmann, M.: Intensität und räumliche Verteilung der Durchwurzelung im Buchenbestand in Abhängigkeit von den Bodenbedingungen auf einer Dauerbeobachtungsfläche, Diploma Thesis, International Forest Ecosystem Management, FH Eberswalde, 2002.
Laruelle, G. G., Roubeix, V., Sferratore, A., Brodherr, B., Ciuffa, D., Conley, D. J., Dürr, H. H., Garnier, J., Lancelot, C., Le Thi Phuong, Q., Meunier, J.-D., Meybeck, M., Michalopoulos, P., Moriceau, B., Ní Longphuirt, S., Loucaides, S., Papush, L., Presti, M., Ragueneau, O., Regnier, P., Saccone, L., Slomp, C. P., Spiteri, C., and Van Cappellen, P.: Anthropogenic perturbations of the silicon cycle at the global scale: Key role of the land-ocean transition, Global Biogeochem. Cy., 23, GB4031, doi:10.1029/2008GB003267, 2009.
Li, H., Jun, H., Wenfeng, T., Hongqing, H., Fan, L., and Mingkuang, W.: Characteristics of micromorphology and element distribution of iron-manganese cutans in typical soils of subtropical China, Geoderma, 146, 40–47, 2008.
Lucas, Y.: The role of plants in controlling rates and products of weathering: Importance of biological pumping, Annu. Rev. Earth Planet. Sci., 29, 135–163, 2001.
Lüttschwager, D. and Remus, R.: Radial distribution of sap flux density in trunks of a mature beech stand, Ann. Sci. Forest., 64, 431–438, 2007.
Madella, M., Alexandre, A., and Ball, T.: International code for phytolith nomenclature 1.0, Ann. Bot., 96, 253–260, 2005.
McKeague, J. A. and Cline, M. G.: Silica in soil solutions I. The form and concentration of dissolved silica in aqueous extracts of some soils, Can. J. Soil Sci., 43, 70–82, 1963.
Mehra, O. P. and Jackson, M. L.: Iron oxide removal from soils and clays by a dithionite-citrate system buffered with sodium bicarbonate, in: Clays and Clay Minerals, edited by: Swineford, A., Proc. 7th Natl. Conf., Washington DC, 1958, Pergamon Press, New York, 317–327, 1960.
Melzer, S. E., Knapp, A. K., Kirkman, K. P., Smith, M. D., Blair, J. M., and Kelly, E. F.: Fire and grazing impacts on silica production and storage in grass dominated ecosystems, Biogeochemistry, 97, 263–278, 2010.

BGD
9, 18865–18906, 2012

Melzer, S. E., Chadwick, O. A., Hartshorn, A. S., Khomo, L. M., Knapp, A. K., and Kelly E. F.: Lithological controls on biogenic silica cycling in South African savanna ecosystems, Biogeochemistry, 108, 317–334, doi:10.1007/s10533-011-9602-2, 2012.

Opfergelt, S., Cardinal, D., Andre, L., Delvigne, C., Bremond, L., and Delvaux, B.: Variations of δ^{30}Si and Ge/Si with weathering and biogenic input in tropical basalt ash soils under monoculture, Geochim. Cosmochim. Ac., 74, 225–240, 2010.

Patel-Sorrentino, N., Lucas, Y., Eyrolle, F., and Melfi, A. J.: Fe, Al and Si species and organic matter leached off a ferrallitic and podzolic soil system from Central Amazonia, Geoderma, 137, 444–454, 2007.

Pavlov, M. B.: Bioelement-Inventur von Buchen- und Fichtenbeständen im Solling, Göttinger Bodenkundliche Berichte, 25, 1–174, 1972.

Puhlmann, M. and Jochheim, H.: Implementation of a multi-layer soil model into Biome-BGC-calibration and application, EOS Transactions Supplement, 88, B24A-05, 2007.

Saccone, L., Conley, D. J., Koning, E., Sauer, D., Sommer, M., Kaczorek, D., Blecker, S. W., and Kelly, E. F.: Assessing the extraction and quantification of amorphous silica in soils of forest and grassland ecosystems, Eur. J. Soil Sci., 58, 1446–1459, 2007.

Sauer, D., Saccone, L., Conley, D. J., Herrmann, L., and Sommer, M.: Review of methodologies for extracting plant-available and amorphous Si from soils and aquatic sediments, Biogeochemistry, 80, 89–108, 2006.

Schachtschabel, P. and Heinemann, C. G.: Wasserlösliche Kieselsäure in Lößböden, Z. Pflanzenern. Bodenk., 118, 22–35, 1967.

Schlichting, E., Blume, H. P., and Stahr, K.: Soils Practical (in German), Blackwell, Berlin, Wien, Germany, Austria, 1995.

Schwertmann, U.: Differenzierung der Eisenoxide des Bodens durch Extraktion mit Ammoniumoxalat Lösung, Z. Pflanzenern. Bodenk., 105, 194–202, 1964.

Soil Survey Staff: Soil Taxonomy – A basic system of soil classification for making and interpreting soil surveys, USDA-NRCS, Agriculture Handbook 436, available at: http://soils.usda.gov/technical/classification/taxonomy, last access: 1 September 2012, 1999.

Sommer, M., Kaczorek, D., Kuzyakov, Y., and Breuer, J.: Silicon pools and fluxes in soils and landscapes – a review, J. Plant Nutr. Soil Sci., 169, 310–329, 2006.

Steinhoefel, G., Breuer, J., Blanckenburg, F., Horn, I., Kaczorek, D., and Sommer, M.: Micrometer silicon isotope diagnostics of soils by UV femtosecond laser ablation, Chem. Geol., 286, 280–289, 2011.

BGD
9, 18865–18906, 2012

Stoops, G.: Guidelines for analysis and description of soil and regolith thin sections, Soil Sci. Soc. Am., Madison, WI, 2003.
Struyf, E. and Conley, D. J.: Silica: an essential nutrient in wetland biogeochemistry, Front. Ecol. Environ., 7, 88–94, doi:10.1890/070126, 2009.
Struyf, E. and Conley, D. J.: Emerging understanding of the ecosystem silica filter, Biogeochemistry, 107, 9–18, 2012.
Struyf, E., Opdekamp, W., Backx, H., Jacobs, S., Conley, D. J., and Meire, P.: Vegetation and proximity to the river control amorphous silica storage in a riparian wetland (Biebrza National Park, Poland), Biogeosciences, 6, 623–631, doi:10.5194/bg-6-623-2009, 2009.
Thornton, P. E., Law, B. E., Gholz, H. L., Clark, K. L., Falge, E., Ellsworth, D. S., Golstein, A. H., Monson, R. K., Hollinger, D., Falk, M., Chen. J., and Sparks, J. P.: Modelling and measuring the effects of disturbance history and climate on carbon and water budgets in evergreen needle leaf forests, Agr. Forest Meteorol., 113, 185–222, 2002.
Trendelenburg, R. and Mayer-Wegelin, H.: Das Holz als Rohstoff, Hanser, München, 1955.
Wanner, M.: A review on the variability of testate amoebae: methodological approaches, environmental influences and taxonomical implications, Acta Protozool., 38, 15–29, 1999.
Watteau, F. and Villemin, G.: Ultrastructural study of the biogeochemical cycle of silicon in the soil and litter of a temperate forest, Eur. J. Soil Sci., 52, 385–396, 2001.
Wilding, L. P. and Drees, L. R.: Biogenic opal in Ohio soils, Soil Sci. Soc. Am. Proc., 35, 1004–1010, 1971.
WRB-World reference base for soil resources, World Soil Resources Reports, 103, p. 128, Rome, FAO, 2006.

BGD
9, 18865–18906, 2012

Table 1. Mineralogical composition (wt.-%) of soil horizons and sediment layers by semiquantative X-ray diffraction.

depth (cm)	quartz	feldspar	pyroxene
0–10	97.1	2.5	0.4
10–20	96.0	3.6	0.4
20–30	97.2	2.5	0.3
30–60	97.7	1.8	0.5
60–80	96.5	3.0	0.5
80–100	93.0	6.6	0.4
100–130	97.4	2.1	0.5
240–260	97.4	2.6	nd
480–500	98.0	2.0	nd

BGD
9, 18865–18906, 2012

Table 2. Phytoliths and related Si pool; n.a. = not assignable.

		depth [cm]	bulk density [Mg m^{-3}]	phytolith [g kg^{-1}]	phytolith [g m^{-2}]	Si content [g kg^{-1}]	phytolith Si, calculated [g kg^{-1}]	phytolith Si, calculated [g m^{-2}]	count-% of total phytolith number (10 SEM micrographs)				
									grasses	beech	mosses	pine	n.a.
litterfall	leaves	–		5.1	–	4.4	2.4	–					
(May–Aug 08)	bud scales	–		7.0	–	3.6	3.3	–					
	fruit capsules	–		1.1	–	1.1	0.5	–					
	branches	–		1.0	–	1.4	0.5	–					
soil	litter layer (L)			8.7			4.1		7	12	4	1	75
	AE	0–2	0.92	0.9	17		0.4	8	16	5	5	3	72
	Ah	2–10	0.99	1.2	92		0.5	43	44	0	1	2	53
	AB	10–20	1.17	0.3	32		0.1	15	45	0	0	1	54
	sum	0–20			140			66					

BGD
9, 18865–18906, 2012

Table 3. Si pools of idiosomic testate amoebae; mean values and standard deviation (in brackets), $n = 5$ field replicates.

depth (cm)	bulk density [$Mg\,m^{-3}$]	living $mg\,Si\,m^{-2}$	empty shells $mg\,Si\,m^{-2}$	total $mg\,Si\,m^{-2}$
0–2.5	0.10 (0.04)	81 (110)	54 (48)	135 (158)
2.5–5	0.36 (0.11)	34 (25)	22 (11)	57 (23)
sum 0–5		116 (106)	76 (43)	192 (148)

BGD
9, 18865–18906, 2012

Table 4. Pools and increments of plant biomass, Si concentrations (mass weighted mean values), Si pools in aboveground biomass, Si fluxes with increment of tree biomass; [a]: calculated from litter fall of May 2006–April 2010; [b]: calculated from stem volume of 2010 or stem growth of 2006–2009; no. in brackets = std.dev. (n = 4 yr).

	biomass pools ($t\,DM\,ha^{-1}$)	litterfall/ increment ($t\,DM\,ha^{-1}\,yr^{-1}$)	Si content ($mg\,kg^{-1}$)	Si pools ($kg\,ha^{-1}$)	Si fluxes ($kg\,ha^{-1}\,yr^{-1}$)
leaves	3.4	3.4 (0.30)	8952 (3101)	29.7	29.7 (7.5)
bud scales	0.5	0.5 (0.04)	2395 (431)	1.2	1.2 (0.3)
beechnuts	0.7	0.7 (0.80)	280 (252)	0.2	0.2 (0.3)
fruit capsules	1.6	1.6 (1.20)	913 (275)	1.4	1.4 (1.1)
other		0.1 (0.03)	10229 (2979)		0.6 (0.4)
branches/twigs including bark		0.4 (0.30)	1649 (183)		0.7 (0.5)
total litterfall		6.7			33.7
branch wood without bark	24.4	0.4	17	0.4	0.01
stem wood without bark	196.1	3.1	17	3.4	0.05
bark of branch wood	2.0	0.0	2565	5.2	0.08
bark of stem wood	16.3	0.2	2565	41.9	0.59
dendromass increment		3.7			0.70
aboveground biomass	245.0			83.4	

BGD
9, 18865–18906, 2012

Table 5. Water fluxes, Si concentrations, and Si fluxes in water (m = measurements, s = simulation); all fluxes are expressed as mean annual values for a four year period (May 2007–April 2011), number in brackets = std.dev (n = 4 yr).

	water flux ($l\,m^{-2}\,yr^{-1}$)	Si concentr. ($mg\,l^{-1}$)	Si flux ($kg\,ha^{-1}\,yr^{-1}$)
precipitation (m)	689 (195)	0.1 (0.03)	0.6 (0.2)
leaching from canopy (m)			0.3 (0.1)
canopy evaporation (s)	168 (28)		
transpiration (s)	239 (24)		
evapotranspiration (s)	476 (62)		
throughfall (m)	491 (189)	0.1 (0.04)	0.8 (0.3)
stemflow (m)	32 (13)	0.3 (0.03)	0.1 (0.0)
stand precipitation (m)	523 (203)		0.9 (0.3)
drainage from 20 cm (s)	316 (152)	4.9 (0.20)	15.4 (7.6)
drainage from 70 cm (s)	262 (139)	5.3 (0.30)	13.9 (8.0)
drainage from 250 cm (s)	**214 (133)**	**5.7 (0.60)**	**12.3 (7.9)**

BGD
9, 18865–18906, 2012

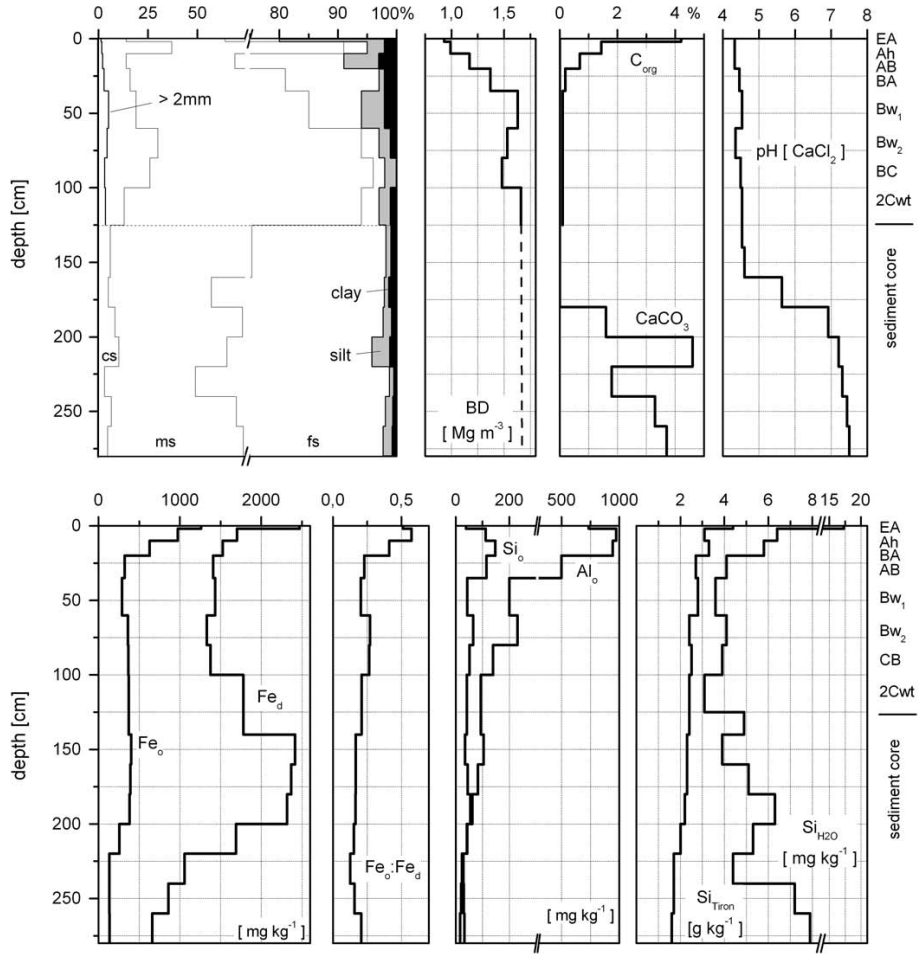

Fig. 1. Depth functions of basic soil properties from the *Brunic Arenosol (dystric)*.

BGD
9, 18865–18906, 2012

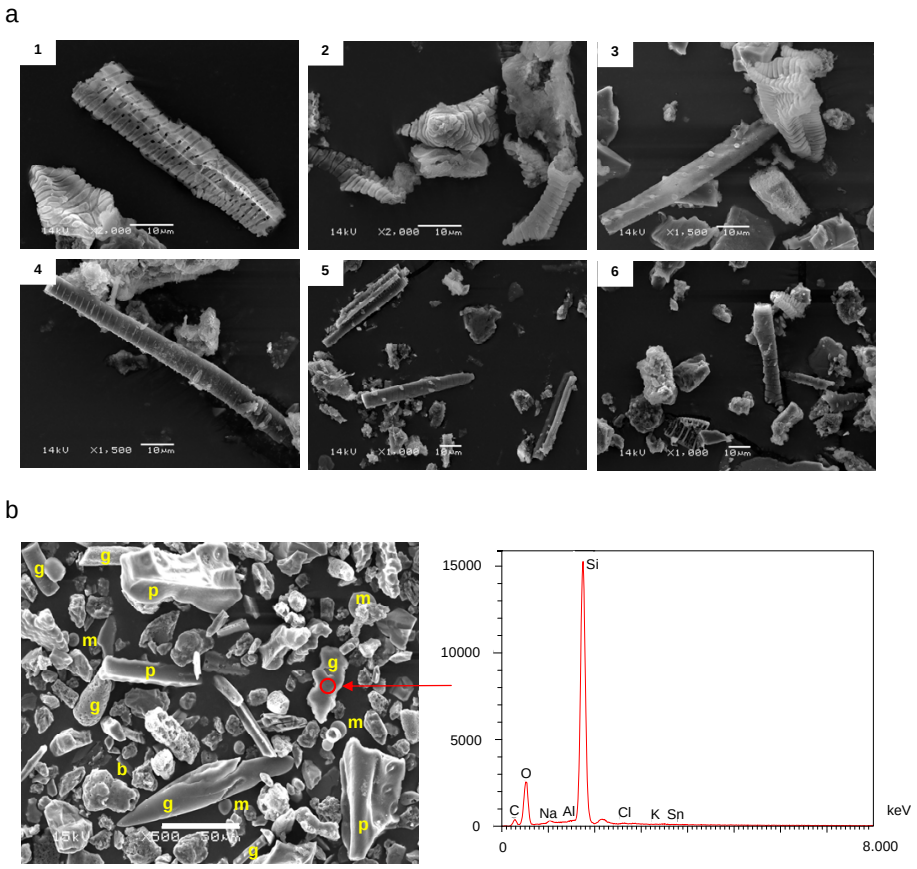

Fig. 2. (a): SEM micrographs of opal phytoliths in *Fagus sylvatica* litterfall (1, 2, 3 leaves, 4, 5 bud scales, 6 fruit capsules), scale bars at all micrographs = 10 µm; **(b)**: SEM micrographs of opal phytoliths in AE horizon, 0–2 cm, scale bar = 50 µm (b = beech, p = pine, g = grass, m = moss); **(c)**: element distribution of a grass opal phytolith (SEM-EDX).

BGD
9, 18865–18906, 2012

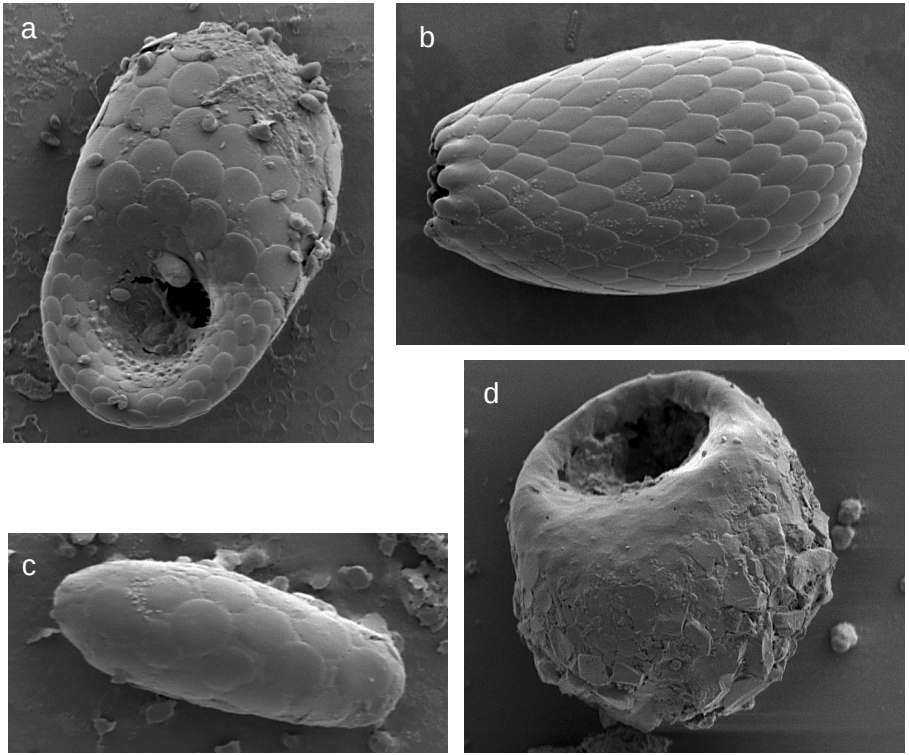

Fig. 3. SEM micrographs of dominant testate amoebae; idiosomic taxa: **(a)**: *Trinema complanatum* (length = 46 µm), **(b)**: *Euglypha rotunda* (length = 49 µm), **(c)**: *Trinema lineare* (length = 23 µm); xenosomic taxa: **(d)**: *Centropyxis sphagnicola* (length = 65 µm).

BGD
9, 18865–18906, 2012

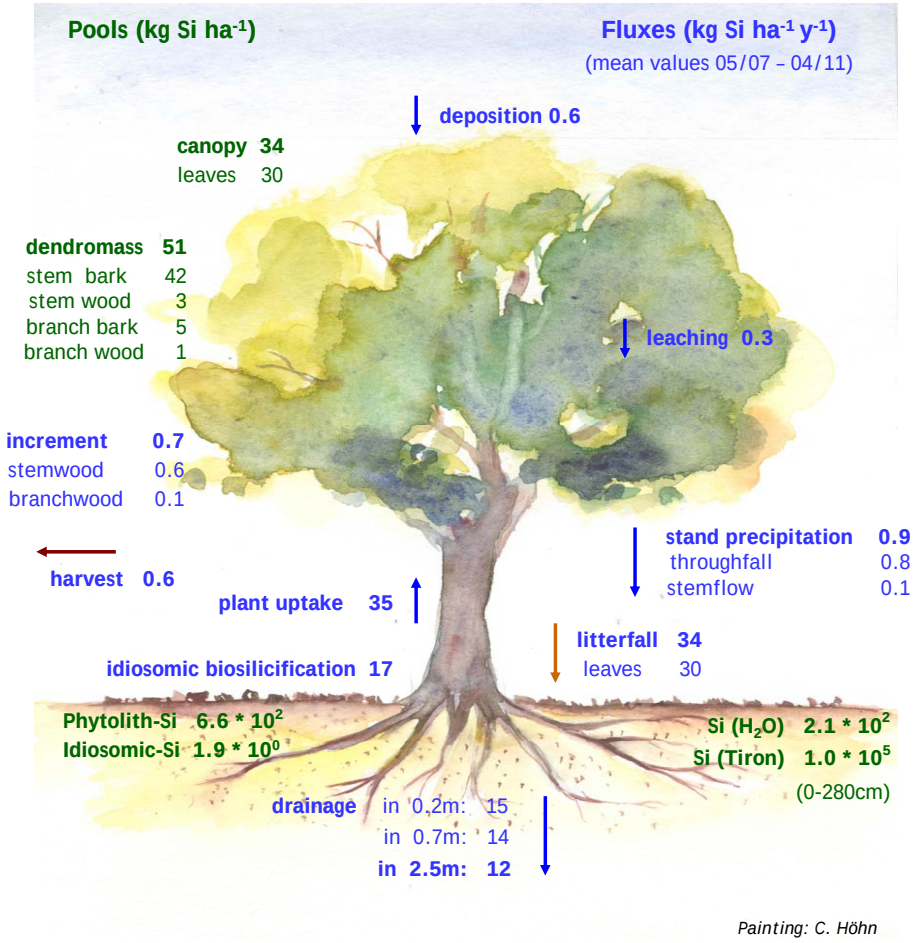

Fig. 4. Si pools and fluxes in the beech-Arenosol biogeosystem "Beerenbusch" (mean values May 2007–April 2011).

BGD
9, 18865–18906, 2012

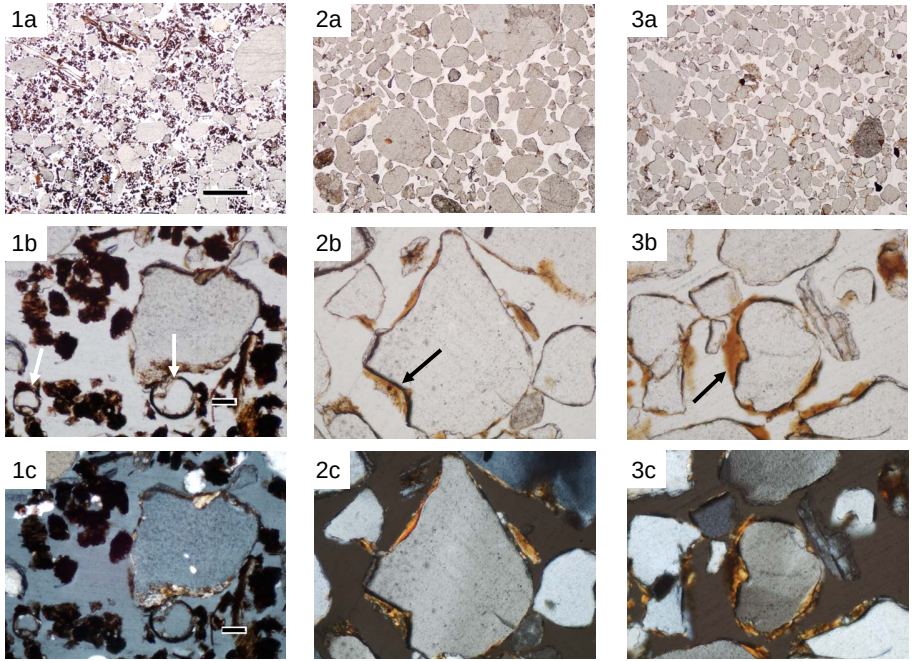

Fig. 5a. Micromorphological properties of soil horizons; microstructure (a, b = PPL, c = XPL) of selected soil horizons: (1) AE (0–2 cm), arrows point to testate amoebae; (2) Bw_1 (44–51 cm), arrow points to Fe-oxides/clay coating; (3) 2Cwt (104–112 cm), arrow points to Fe-oxides/clay coating; widths of photo: 1a, 2a, 3a = 6 mm; other = 0.6 mm.

BGD
9, 18865–18906, 2012

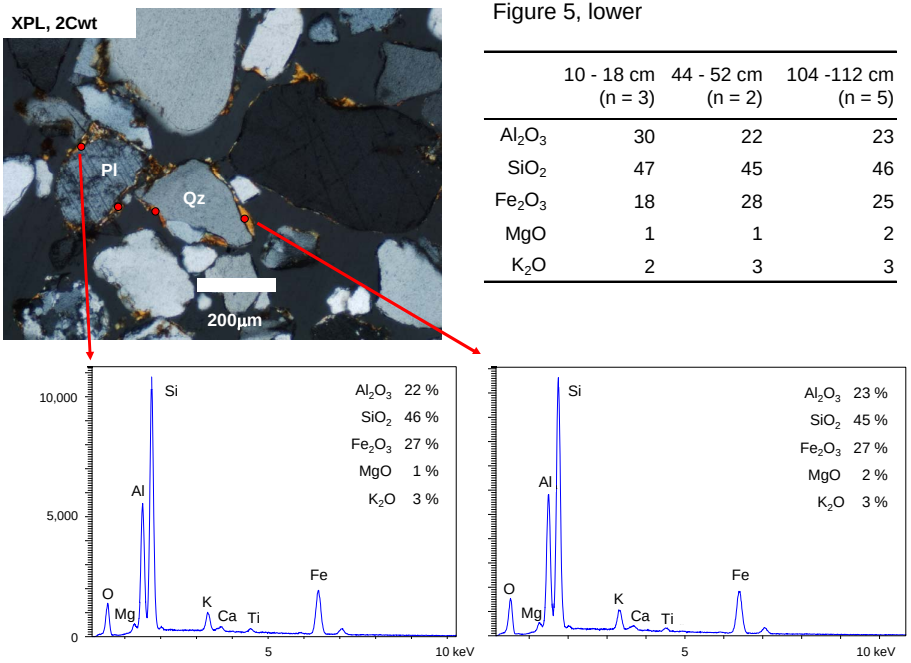

Figure 5, lower

	10 - 18 cm (n = 3)	44 - 52 cm (n = 2)	104 -112 cm (n = 5)
Al_2O_3	30	22	23
SiO_2	47	45	46
Fe_2O_3	18	28	25
MgO	1	1	2
K_2O	2	3	3

Fig. 5b. SEM-EDX micrographs of cutans in 2Cwt (104–112 cm); average chemical composition (wt.-%) of coatings of different depths analysed by electron microprobe; number in brackets = no. of cutans analysed by EDX in each thin section.

BGD
9, 18865–18906, 2012

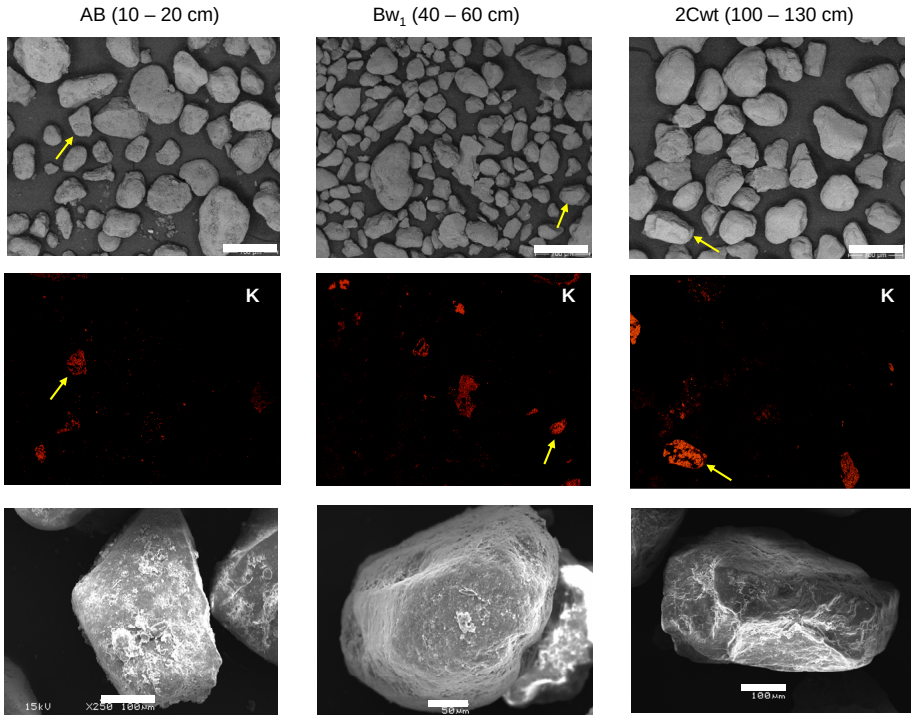

Fig. 6. SEM-micrographs and EDX element mapping (K) of soil material (< 2 mm) from three different depths; scale bars: upper row = 700 µm; lower row, left and right = 100 µm, middle = 50 µm; yellow arrows point to orthoclase mineral grains shown in lower row.

BGD
9, 18865–18906, 2012

Figure 7

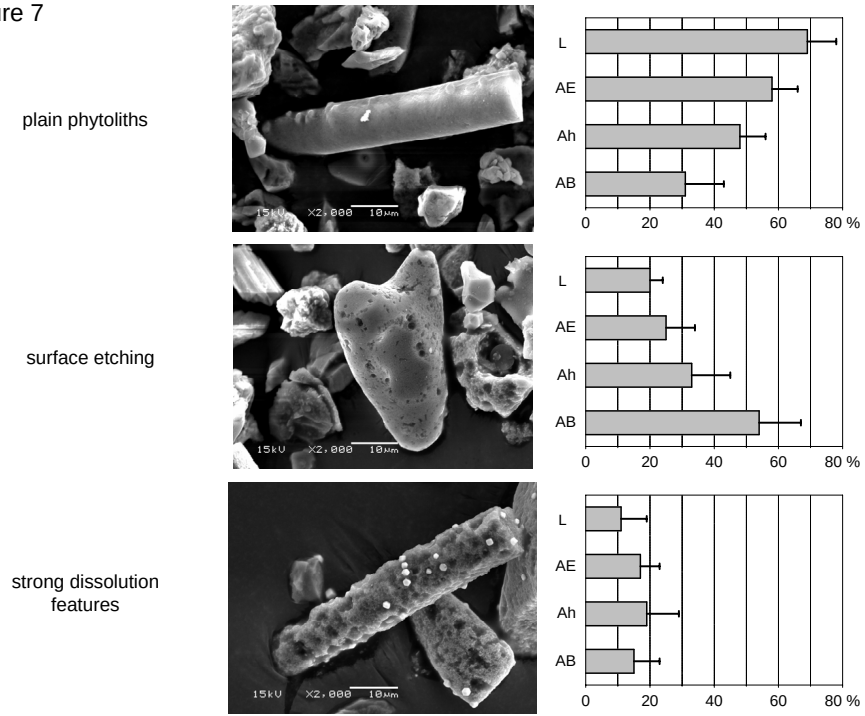

Fig. 7. Categories and depth functions of phytolith dissolution (based on counting in SEM micrographs): fresh, plain phytoliths (upper), phytoliths showing clear signs of surface etching (middle), and phytoliths showing strong dissolution features (lower); horizontal bars = mean ± SD (n = 10 micrographs), total number of phytoliths counted: O = 462, AE = 459, Ah = 422, AB = 238.

BGD
9, 18865–18906, 2012